Available online at www.sciencedirect.com
ScienceDirect
Bioelectrochemistry 70 (2007) 320–327
Bioelectrochemistry
www.elsevier.com/locate/bioelechem

# Electrostatic properties and macroscopic electrodiffusion in OmpF porin and mutants

Marcel Aguilella-Arzo, Juan J. García-Celma, Javier Cervera, Antonio Alcaraz *, Vicente M. Aguilella

*University Jaume I, Department of Experimental Sciences, Biophysics Unit, P.O. Box 8029, E-12080 Castellón, Spain*

Received 13 February 2006; received in revised form 18 April 2006; accepted 18 April 2006
Available online 29 April 2006

**Abstract**

The bacterial porin OmpF found in the outer membrane of *E. coli* is a wide channel, characterized by its poor selectivity and almost no ion specificity. It has an asymmetric structure, with relatively large entrances and a narrow constriction. By applying continuum electrostatic methods we determine the ionization states of titratable amino acid residues in the protein and calculate self-consistently the electric potential 3-D distribution within the channel. The average electrostatic properties are then represented by an effective fixed charge distribution along the pore which is the input for a macroscopic electrodiffusion model. The theoretical predictions agree with measurements performed under different salt gradients and pH. The sensitivity of reversal potential and conductance to the direction of the salt gradient and the solution pH is captured by the model. The theory is also able to explain the influence of the lipid membrane charge. The same methodology is satisfactorily applied to some OmpF mutants involving slight structural changes but a large number of net charges. The correlation found between atomic structure and ionic selectivity shows that the transport characteristics of wide channels like OmpF and its mutants are mainly regulated by the collective action of a large number of residues, rather than by the specific interactions of residues at particular locations.


*Keywords:* Electrodiffusion; OmpF; Bacterial porin; Channel selectivity

## 1. Introduction

One of the main goals of modern biophysics is to understand the correlation between atomic structure and physiological function. This search is particularly evident in the efforts to unveil the crystallographic structure of a number of biological ion channels. During decades a great deal of information about biochannels was inferred from macroscopic measurements, often using electrophysiology or electrochemistry techniques. The knowledge about their ternary structure was scarce. The situation changed when the crystallographic structure of some ion channels could be determined at atomic resolution. However, even for these channels the connection between their structure and physiological properties is not yet completely understood. This is the case of the bacterial porin OmpF found in the outer membrane of the bacteria *Escherichia coli*, object of numerous recent studies [1,2]. Like other bacterial porins, it can be purified and modified genetically. This makes it an attractive system to test the available theoretical models of channel permeation.

When reconstituted into planar lipid membranes, OmpF porin forms trimeric channels. Studies made under these experimental conditions show that the passage of small inorganic ions through the porin is passively controlled and that long range electrostatic interactions play a fundamental role [3]. However, the translocation of antibiotic molecules is believed to be influenced by hydrophobic interactions at the channel constriction [1,4].

The OmpF system is so complex that currently there is no unique theoretical model that can explain all its transport properties [5]. For this reason, different approaches have been tried on it, each one addressed to a particular aspect. On the one hand, powerful methods such as Molecular Dynamics (MD), Brownian Dynamics (BD) or 3-D Poisson–Nernst–Planck (PNP) have provided fine details about the ion permeation [6–9].

* Corresponding author. Tel.: +34 964 728044; fax: +34 964 728066.
*E-mail address:* alcaraza@exp.uji.es (A. Alcaraz).

1567-5394/$ - see front matter © 2006 Elsevier B.V. All rights reserved.
doi:10.1016/j.bioelechem.2006.04.005

However, they have faced important technical difficulties since OmpF is a poorly selective channel and therefore a large number of correlated ions must be included in the simulation to gather meaningful statistics. On the other hand, mean field theories, such as 1-D PNP or the Teorell–Meyer–Sievers (TMS) theory, have been used to calculate electrodiffusion quantities on this system [3,10]. They commonly use effective parameters which are fitted to the experimental data.

A detailed experimental study of the ionic selectivity of the OmpF porin has been reported recently [3]. In this work, selectivity measurements were analyzed by means of a modified TMS theory. This approach was useful to explain semi-quantitatively the change of the zero current potential (also known as reversal potential) with electrolyte concentration and concentration gradient across the channel. The model made use of adjustable parameters to fit the experimental values. However, no rationalization of these parameters in terms of the microscopic structure of the channel was made. In addition, the model was not used to address questions like the pH dependence of the channel selectivity and conductance. Rather, only tentative correlations between measured reversal potential and the total charge of the channel (estimated by simply counting the number of charged groups) were attempted. The study finally suggested that electrostatic long range interactions were determinant in the transport of small hydrophilic ions.

The present work stresses the importance of the average electrostatic properties of the OmpF porin on its transport characteristics. We show that effective average electrostatic properties obtained directly from the microscopic structure of the protein regulate the ionic transport under a variety of experimental conditions. This conclusion holds also for some engineered OmpF mutants with very different electrostatic properties but similar atomic structure to that of wild type OmpF. To this end, we link the microscopic electric properties of the pore-forming protein with electrodiffusion measurable quantities. This is accomplished by a three-step procedure summarized as follows:

(1) The ionization state of the titratable residues of the channel is determined. This allows us to calculate the electric potential created by the pore fixed charges.
(2) An averaging procedure is used to convert the 3-D electric potential distribution into a 1-D profile of effective fixed charge volume density along the pore.
(3) This 1-D profile is then used as input for a 1-D PNP model. This set of equations is finally solved numerically to obtain electrodiffusion magnitudes which are compared with previously reported experimental data in a wide variety of experimental conditions.

The model outlined above constitutes a macroscopic electrodiffusion theory of the ion transport across the pore, but it is based on microscopic structural information. The usefulness of the model depends on the capability of a 1-D PNP approach with effective magnitudes to describe the transport properties of a system in the nanometer region as is the OmpF porin. Recent studies in both synthetic and biological nanopores support this idea. One dimensional treatments based on Smoluchowski equation, Fick–Jacobs approximation and Poisson–Nernst–Planck equations provide interesting clues for planning more efficient synthetic biosensors, nanopumps and nanodiodes [11–13]. In addition, satisfactory comparisons between mean field theories and Brownian dynamics simulations are found for wide biochannels [14]. In fact, several 1-D PNP approaches describing the ion transport across different biological ion channels have already been reported: The acetylcholine receptor [15], the L-Type calcium channel [16], the calcium release channel [17], the mitochondrial channel VDAC [18,19] or the OmpF porin [3,10] among others. Interestingly, the extensive research done in related areas, like solid state physics and computational electronics, shows that the continuum approach provides reasonable results in many controversial conditions [20–22].

## 2. Formulation of the problem

The electrodiffusion magnitudes are calculated by means of a 1-D PNP theory. This theory uses a mean-field approximation where average ion fluxes are related to concentration and electric potential gradients, and the electric potential is determined by the fixed and mobile charges in the pore. 1-D Nernst–Planck flux equations read:

$$J_i = -D_i\left[\frac{\mathrm{d}c_i(z)}{\mathrm{d}z} + \frac{e}{kT}q_i c_i(z)\frac{\mathrm{d}\phi(z)}{\mathrm{d}z}\right] \tag{1}$$

where $z$ is the coordinate along the symmetry axis of the trimer normal to the membrane [23], $D_i$, $c_i$ and $q_i$ are the diffusion coefficient, the concentration and the charge number of charged species $i$, respectively, $e$ is the elementary charge, $k$ is Boltzmann constant, $T$ is the absolute temperature, and $\phi$ is the local electric potential. The latter includes both the electrical potential applied externally ($V$) and that which arises from the fixed charges of the channel ($\psi$). This electrostatic potential is calculated from the charge density inside the pore using the Poisson equation

$$\frac{\mathrm{d}}{\mathrm{d}z}\left[\varepsilon_s\frac{\mathrm{d}}{\mathrm{d}z}\phi(z)\right] = -\rho_f(z) - eN_A\sum_i q_i c_i(z) \tag{2}$$

where $\varepsilon_s$ is the electric permittivity of the solution, $\rho_f(z)$ is the effective fixed charge density arising from the protein charges and $N_A$ is the Avogadro–Loschmidt constant. The second term in the right-hand side of Eq. (2) represents the mobile charge density owing to free ions in solution. To solve the PNP system the effective fixed charge density of the channel is needed. We now introduce a procedure to estimate this magnitude directly from the microscopic information given by the channel structural data.

Each titratable residue of the channel is in an environment of low electric permittivity (the protein). It interacts with the protein permanent fixed partial charges (due to the different electronegativities of the atoms in the molecule) and with the rest of titratable residues. In addition, these interactions are influenced by the shielding effect of the ions in solution. This implies that the proton dissociation constant $K_a$ (or its equivalent in the logarithmic scale $pK_a$) of the residue inside the

protein is different from that in free solution. Therefore, we need to calculate the p$K_a$ value of each titratable residue inside the protein, which is then known as *apparent* p$K_a$. The protocol followed to perform this calculation has been described previously in detail [3]. It is based on the procedure described by Antosiewicz et al. [24,25]. The UHBD code (the University of Houston Brownian Dynamics Program) [26,27] is employed to perform the calculation using the three-dimensional structure of the OmpF trimer with a resolution of 2.4 Å (Protein Data Bank id. code: 2OMF) as obtained from X-ray analysis [23]. Using the apparent p$K_a$, a rough estimate of the charge density was done by simply counting the charged residues at a given pH [3]. However, using this approach the precise location of the residues and the partial charges of the protein were not considered. All this information is contained in the electric potential profile $\psi(\vec{r})$, what suggests the idea of using $\psi(\vec{r})$ as an indirect means of estimating the effective charge density of the channel.

It has been reported in the literature that it is possible to obtain a 1-D equivalent of a 3-D magnitude by doing averages over the pore cross section[13,28,29]. According to these studies, the procedure provides effective magnitudes that keep their essential physical meaning as long as their local curvature is not too great. The UHBD program calculates the electric potential map at equilibrium by solving the Poisson equation. This equation takes the form of the Poisson–Boltzmann (PB) equation within the aqueous pore region. We have checked that in computations done at physiological ionic strength (as is the case of the present study) the results are unchanged whether the calculations are done taking all the nonlinear terms in the PB equation into account or linearizing the PB equation. Other computational studies performed in the same protein channel report an identical conclusion [30,31]. In the linear approximation, the PB equation can be written as

$$\nabla^2\psi(\vec{r}) = \kappa^2\psi(\vec{r}) \tag{3}$$

where $\kappa$ is the inverse Debye length of the solution. The right hand side of Eq. (3) is the opposite to the charge density arising from the ions in solution, which compensates for the fixed charge of the protein (the calculation is performed at equilibrium). Therefore, the average charge density $\rho_f(z)$ of the protein over a cross sectional slice of constant $z$ can be estimated as

$$\rho_f(z) = \varepsilon_s\kappa^2\bar{\psi}(z) \tag{4}$$

where $\bar{\psi}(z)$ is the average of the electric potential in the cross sectional slice. $\rho_f(z)$ is expected to capture the average electrostatic interaction felt by the ions in solution as they cross the channel. A similar idea can be found in [5]. Note that the relationship between averaged quantities expressed by Eq. (4) is only rigorously correct under the linear approximation of PB equation.

Fig. 1 shows the calculated equipotential lines superimposed over a section of the OmpF monomer. The axial profile of $\rho_f(z)$ is shown at the bottom panel. This average fixed charge density profile can be used as an input parameter to solve self-consistently the 1-D PNP system of equations (Eqs. (1) and (2)) and obtain the electrodiffusion quantities: i.e., the 1-D profiles of electric potential, $\phi(z)$, and ionic concentration, $c_i(z)$. We assume thermodynamic quasiequilibrium at the pore-solution interfaces. The bulk concentrations and the boundary concentrations ($c_i(z=0)$ and $c_i(z=d)$, where $d$ is the pore length) are then related through

$$c_i(0) = c_i^{cis}\left\{1-\frac{e}{kT}q_i\left[\phi(0)-\phi^{cis}\right]\right\} \tag{5a}$$

$$c_i(d) = c_i^{trans}\left\{1-\frac{e}{kT}q_i\left[\phi(d)-\phi^{trans}\right]\right\} \tag{5b}$$

where *cis* and *trans* refer to bulk solutions next to $z=0$ and $z=d$, respectively,and the externally applied potential is $V=\phi^{cis}-\phi^{trans}$.

The relationship between boundary conditions and bulk concentration expressed in Eqs. (5a) (5b) is equivalent to assuming Donnan equilibria on both channel solution interfaces. This approximation is widely accepted for synthetic membranes and nanopores which are in the micrometer thickness range [32,33]. However, when the membrane is very thin as is the case of biological membranes (nanometers), the use of this boundary condition is controversial. A contribution by Gillespie and Eisenberg [34] that tackles this question concludes that the usual treatment of the Donnan potential gives the correct value for the electrodiffusion magnitudes despite the obtained profiles of concentration and electric potential may not be accurate.

An iterative relaxation method is used to solve the PNP equations [35]. The effective charge distribution is mapped into a grid of 500 equally spaced points. For a given applied voltage, an initial guess for the potential profile is evaluated just using a

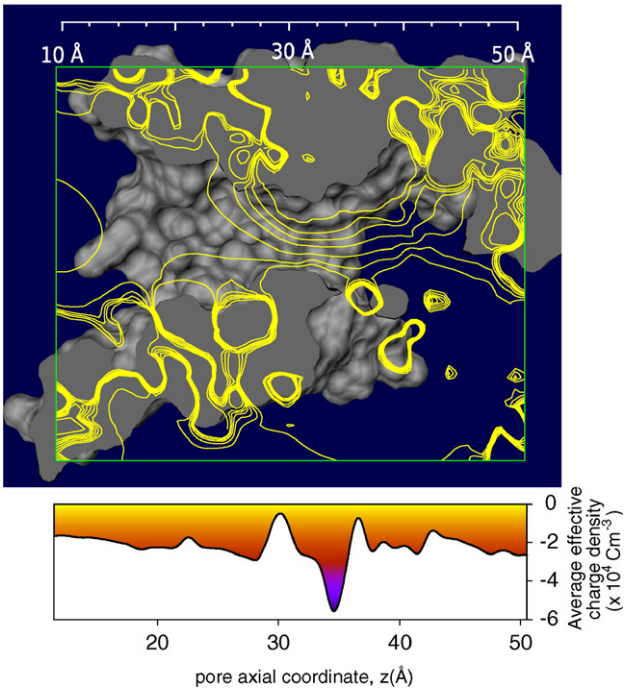


Fig. 1. Calculated equipotential lines superimposed over a section of the OmpF monomer (the plane is defined by the atoms Lys10-C157, Thr165-C2439 and Asp206-O3933). The profile of the effective fixed charge density along the channel is shown below.

linear approximation. This solution is then iterated until a tolerance of $10^{-10}$ is fulfilled. The outputs of the numerical procedure are the ionic flux densities $J_+$ and $J_-$ for a given applied voltage. From these values, the current can be obtained as $I=\pi a^2 F(J_+-J_-)$, where $a$ is the effective radius of the channel.

## 3. Results and discussion

The underlying idea of this work is that ion selectivity of wide channels is determined mainly by average electrostatic properties rather than by the particular 3-D charge distribution. To this end, our simple continuum model aims to reproduce the main channel features under different experimental conditions of salt concentration and pH.

The protein electric permittivity is set at $\varepsilon_m=20$ and the solution electric permittivity at $\varepsilon_s=80$ [3,24,25,30]. The calculation of p$K_a$ values and $\psi(\vec{r})$ is performed using 50 mM as electrolyte concentration to avoid the shielding effects. This concentration value is not critical. Calculations performed by Varma and Jakobsson [30] show that ionization states at neutral pH are unchanged whether the calculations are done at physiological concentrations or even using almost zero ionic strength. The free solution diffusion coefficients are used. Some MD simulations in OmpF give smaller cation and anion diffusion coefficients [7,8] but with the same ratio between them. Therefore, this should not affect our calculations. Finally, an effective radius of 0.6 nm is used. This value is close to the average radius of the channel constriction (presumably the rate limiting step for ion migration across the pore).

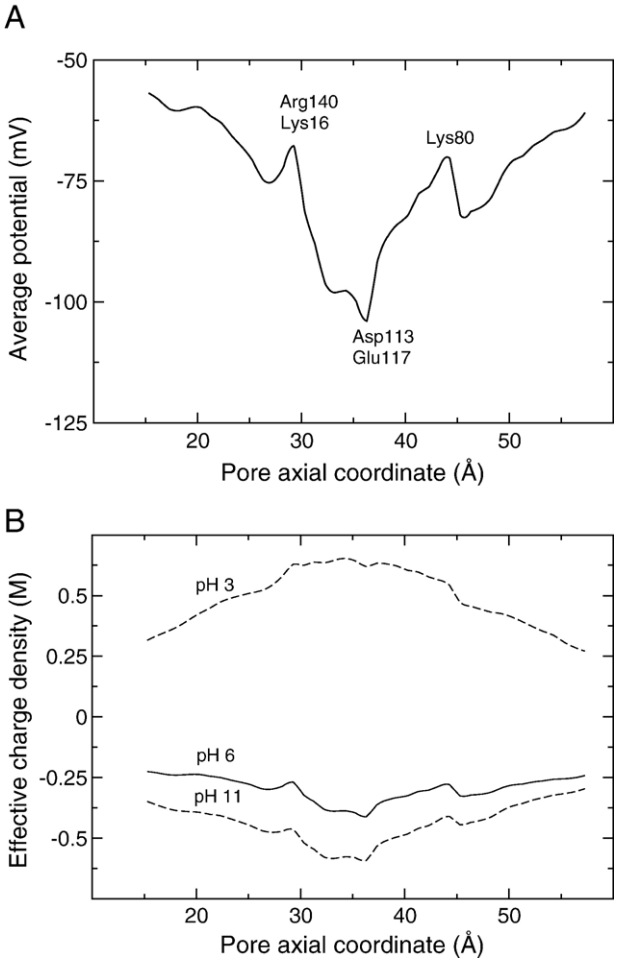


Fig. 2. (A) Model calculations of the electric potential profile along the pore longitudinal axis for an OmpF channel in KCl solution. The potential at each axial position is the averaged value over the solvent-accessible region of every channel cross-section. Labels with the main ionizable residues to which the principal peaks and wells may be ascribed are included. (B) Average effective fixed charge density along the pore. Negative charge at neutral and basic pH is consistent with the cation selectivity of OmpF and positive charge in very acidic solutions agrees with the observed anion preference of the channel.

### 3.1. Average electrostatic properties of the wild-type OmpF porin

The calculated transport properties of OmpF porin depend on the selection of the information in the averaging process. Therefore, it is advisable to have a look at the averaged electric potential to see if it retains the basic features of the channel.

Fig. 2A shows the axial profile of between $z=16$ Å and $z=58$ Å at pH 6. The cation selectivity of the channel at pH 6 is a consequence of the negative potential throughout the entire pore. The depth of the potential well at the channel constriction is around $4kT$ ($\approx$100 mV) in accordance with other calculations [3,36]. While the resulting profile averages the influence of a large number of residues (over 100), we may try a tentative assignment of peaks and wells to some specific residues. The objective is to see the consistency of $\bar{\psi}(z)$ with the crystal structure. In this way, the peak around $z=29$ Å can be ascribed to the positively charged Arg140 and Lys16. The negative residues of the constriction Asp113 and Glu117 would be responsible for the well around $z=36$ Å. Finally, the peak around $z=43$ Å would be ascribed to Lys80.

We consider next the pH dependence of the channel selectivity as reported experimentally [37]. Fig. 2B shows the calculated effective charge concentration profile along the pore at different values of the solution pH. At high and neutral pH, $\rho_f(z)$ attains negative values which are consistent with the cation selectivity that exhibits the OmpF channel [3,37,38]. At very low pH, however, the model predicts a positive $\rho_f(z)$ in accordance with the switch of OmpF selectivity to anionic in the presence of very acidic solutions.

### 3.2. Response of measured channel selectivity to pH changes

In the previous section the model was shown to qualitatively describe the selectivity of OmpF for different pH values. However, to test the assumptions made in the model a quantitative comparison with experimental data must be done. The selectivity of a channel is usually quantified in terms of the reversal potential. For this reason, the model predictions for the reversal potential are here compared to experimental data in different situations.

In Fig. 3 we present reversal potential measurements (previously reported in [3]) together with the theoretical predictions for the same conditions (triangles). The series correspond to a tenfold ratio of bulk KCl concentrations ($c_{cis}=1$ M and $c_{trans}=0.1$ M) at different pH (the same in both solutions). The reference value

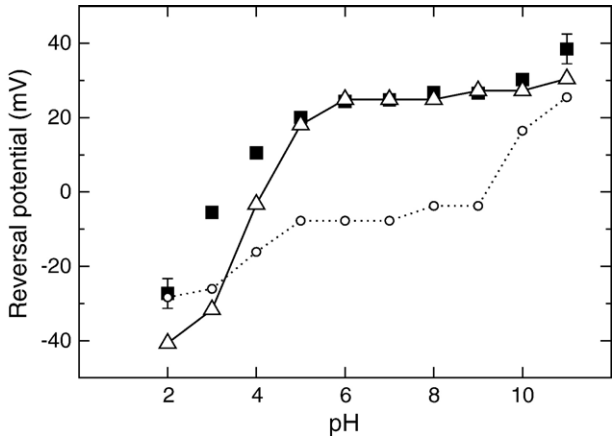


Fig. 3. Experimental (squares) and theoretical prediction (triangles) of the reversal potential for KCl $c_{cis}=1$ M | $c_{trans}=0.1$ M as a function of the pH. Good agreement is found between theory and experiments but for extreme pH conditions. The reversal potential predicted exclusively by the residues at the channel constriction (circles) is also shown. In this case, the model predicts an anion selective channel for most of the pH range. Lines are shown to guide the eye.

for the electric potential is on the *trans* side ($V^{bulk}=0$). The model accounts for the increase of the reversal potential with pH: the anion selectivity of the channel at very acidic pH turns into almost no selectivity at pH 4 and reaches a plateau of cation selectivity in the region between pH 6 and 9. It is remarkable that such a simple model is able to account for the OmpF selectivity over a broad pH range. Good agreement between theory and experiment is found except for extreme pH values. The deviations at low and high pH values are expected if we consider that under such conditions the $H^+$ or $OH^-$ concentration may become comparable to that of salt in the low concentrated solution, a situation which has not been considered in the PNP system. In addition, we may speculate that the changes in the protonation states of a large number of residues may alter the porin structure. The results obtained indicate that the dependence of the channel selectivity with pH can be explained by the combined action of all the channel residues.

The question that arises now is whether this dependency can be explained equally well using only the protonation state of crucial residues at the channel eyelet. If this were the case, the central constriction of the channel would act as its *selectivity filter*. It has been shown previously [3,36] that the channel constriction contains up to seven basic residues with estimated p$K_a$s around 13–15: the so-called cluster of arginines [23], one lysine and three tyrosines. In addition, there are two acidic residues, one aspartic acid and one glutamic acid with calculated p$K_a$s around 3 and 6, respectively. At neutral pH all these residues are charged. Therefore, taken independently from the rest of residues, the central constriction would display an excess of positive charge which would be unable to explain the cation selectivity of the channel [37]. To address quantitatively this issue, we cut off the channel leaving only the residues placed in the channel constriction. The whole procedure, including the p$K_a$ calculation, was performed to obtain the reversal potential due exclusively to the residues at the constriction. The results are also shown in Fig. 3 (circles). As expected, the calculations predict unrealistic values. From these results one could come to the wrong conclusion that the channel is anion selective except for extreme basic conditions (pH>8).

### 3.3. Non-uniform charge distribution and reversal potential

The orientation of the OmpF porin reconstituted in the lipid membrane is mostly unidirectional in the experiments here reported [3] and the reversal potential depends on the direction of the concentration gradient. This is observed when the reversal potential is measured for a given ratio $c_{cis}/c_{trans}$ and its inverse $c_{trans}/c_{cis}$. For a totally symmetric channel the two experiments must give the same reversal potential value, but with opposite sign. However, this is not the case for the OmpF channel probably because it is asymmetric in the structure and the fixed charge distribution [23,36]. This feature allows us to see how the model accounts for the asymmetry of the OmpF channel. Interestingly, this is not just an anecdotic characteristic of this channel. In fact, a similar effect has been reported in conical synthetic nanopores and proves that it is possible to use it as a basis to construct ionic nanofilters [13].

Fig. 4 shows the results of reversal potential measurements for a wide range of concentration ratio values. The solid line represents the model prediction. The model reproduces the asymmetry found in reversal potential measurements, although it underestimates it. Compare for example the reversal potential for KCl in 3 M (*cis*) | 0.1 M (*trans*) vs. 0.1 M (*cis*) | 3 M (*trans*). This reduction probably means that the averaging process levels off part of the inherent asymmetry of the system. Despite this fact, it can still be inferred that the asymmetry of the channel selectivity naturally arises from the non-homogeneity of the channel in the axial direction, and that this channel feature is partially maintained in the averaging procedure (performed for every cross section).

### 3.4. Change of channel conductance with concentration and voltage bias

The OmpF channel conductance is known to be pH dependent and slightly voltage dependent, particularly at low salt

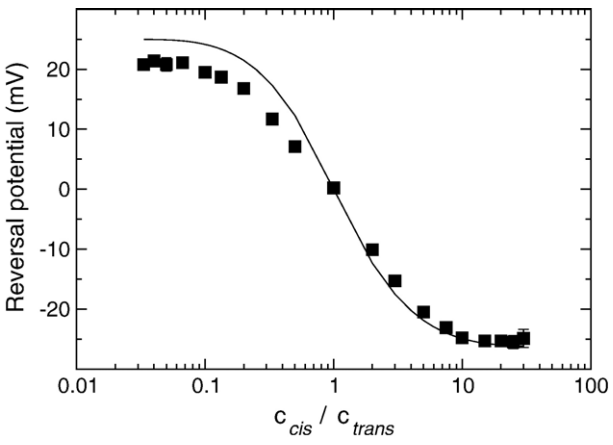


Fig. 4. Change of OmpF reversal potential with salt concentration ratio in KCl solutions at pH 6. The lower electrolyte concentration was kept at 0.1 M while the higher concentration was changed to obtained the desired concentration ratio. The solid line denotes the model calculation, which predicts the sign of the reversal potential asymmetry but underestimates its magnitude.

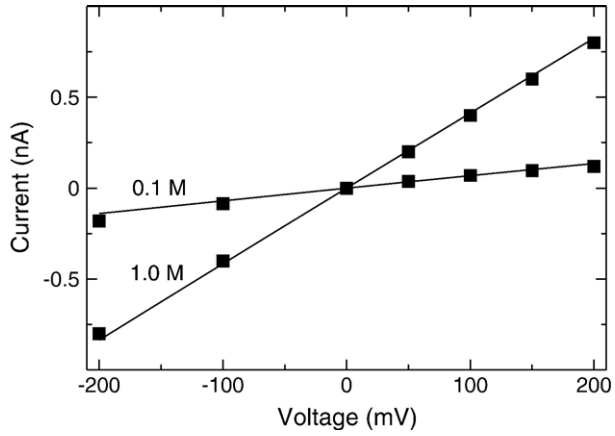


Fig. 5. Experimental (squares) and theoretical (solid lines) current–voltage curves for two KCl electrolyte solutions. The model correctly predicts the change in the slope of the curves.

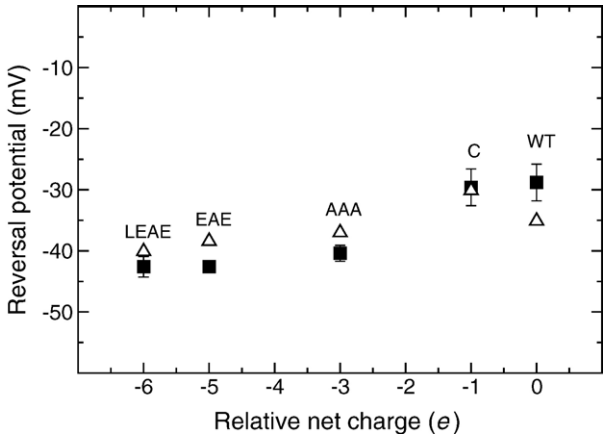


Fig. 7. Measurements (squares) and model calculation (triangles) of the reversal potential of wild type (WT) OmpF and four mutants. Mutations involved slight structural changes but a high variation in net charge.

concentration [37]. These dependences arise from the charge regulation with pH and from the asymmetry of the channel. Unlike the reversal potential, now the model has to reproduce a complete current–voltage curve rather than a single point (zero current potential).

Fig. 5 shows the experimental current–voltage curves (squares) and the theoretical predictions (triangles) at pH 6 in 0.1 M and 1 M KCl solutions. The agreement theory-experiment is reasonably good. The change in the current–voltage curve with the concentration is well described by the model. It depends on a combined effect of the increase of ionic concentration and the shielding effect of the electrolyte. The latter is accounted for by the PNP system in the model, what reinforces the view that the transport is determined by long-range electrostatic interactions. In addition, the model also displays the asymmetry observed experimentally, although the predicted one is smaller. Note that the same occurred when the reversal potential was considered.

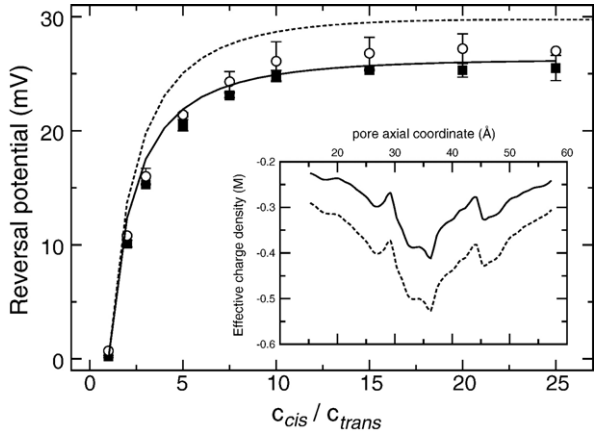


Fig. 6. OmpF reversal potential measurements in DPhPS negatively charged membranes (circles) and DPhPC neutral membranes (squares). Model predictions for a neutral membrane (solid line) and for a charged membrane (dashed line) are shown. Experiments were done at pH 6 and keeping the *trans* side concentration at 0.1 M KCl. The inset shows the average effective charge for the neutral (solid line) and the charged membrane (dashed line).

### 3.5. Influence of the charge of the lipid bilayer

The charge of the lipid used in the formation of planar lipid bilayer influences the measured transport properties of the OmpF [3]. This feature has been observed in reversal potential and conductance measurements. When planar membranes were formed from negatively charged lipids, diphytanoylphosphatidylserine (DPhPS), the absolute value of the reversal potential at pH 6 was higher than when neutral lipids, diphytanoylphosphatidylcholine (DPhPC), were used. The same tendency was observed in the conductance, especially at low concentration.

For the sake of simplicity, the charge of the lipid was included in the theory as an effective charge density in the form of partial charges in the spheres that model the polar heads of the lipid bilayer. It was also assumed that the p$K_a$ values of the protein residues were not affected by the charge of the membrane.

Fig. 6 shows the OmpF reversal potential measured in DPhPS negatively charged membranes (circles) and the DPhPC neutral membranes (squares) together with the model prediction for a neutral membrane (solid line) and for a membrane with an effective charge density of $-1e/9$ nm$^2$ (dashed line). The measurements were made at pH 6 for 0.1 M KCl in the *trans* side and varying the concentration in the *cis* side. The average effective charge concentration for the neutral membrane (solid line) and the charged one (dashed line) is shown as an inset. The model accounts for the increase in the reversal potential when the membrane is charged. Therefore, we can hypothesize that the negative charge of the bilayer is added to that of the channel to increase its cation selectivity. This effect is reflected in the model through the increase of the effective charge density. Note however that the change in reversal potential might be driven by other effects. For instance, the surface tensions of a charged bilayer and a neutral one are different. This could affect the curvature of the bilayer close to the channel mouths as well as the channel structure since the pressure exerted by the bilayer is different in both cases.

### 3.6. Average electrostatic properties and the study of OmpF mutants

A recent paper by Miedema and coworkers [39] provides some extra clues to understand ion selectivity of the OmpF porin. The protein was manipulated by changing some crucial residues at the channel lumen so that the weakly selective OmpF was turned into a $Ca^{2+}$ selective channel. On the light of a charge/space competition model, the authors came to the conclusion that the fixed charge density was the key determinant of ion selectivity, with the precise atomic arrangement having only second-order effects. As we suggest similar ideas here, our model can be challenged with some of the results obtained with these manipulated proteins.

We consider four mutants studied by Miedema et al.: the C mutant (one mutation providing one extra negative charge), the AAA mutant (three mutations providing $-3e$ extra charge), the EAE mutant (three mutations providing $-5e$ extra charge) and finally, the LEAE mutant (four mutations providing $-6e$ extra charge) (see Table 1 of Reference [39] for details). The crystal structures of these mutants have not been resolved yet. However, since in their mutations only a small number of aminoacids were changed, it is expected that they conserve the structure of the wild type OmpF to a large extent [30].

Model structures were obtained by simply substituting the side chains of the implicated residues. The structures were then relaxed using GROMACS [40]. 500 steps were performed to minimize the energy of the protein by means of the Steepest Descent method.

In Fig. 7 we present the reversal potential recorded for each mutant and the wild type OmpF (WT) for a 10-fold gradient (1.0 M | 0.1 M KCl) as reported in [39] (squares). The model prediction is also shown (triangles). A good agreement is found between theory and experiments. Note that the discrepancies between the theory and experiments (~ 5 mV) are of the order of those found between different experiments performed with wild type OmpF using different protocols[3,39]. This indicates that the procedure is also valid for mutants involving a relatively large number of net charges and, accordingly, a high selectivity. This extension implies that average properties are sufficient to determine the reversal potential.

## 4. Summary and conclusions

A theoretical model for the electrodiffusion across the OmpF channel and some of its mutants has been developed. It is based in the PNP system of equations. However, no free parameters have been used to fit the experimental data. Instead, a procedure to link the microscopic information to an effective charge density that allows for the solution of the PNP system has been introduced. The procedure takes advantage of the available crystallographic structure at atomic resolution. It starts by inserting the OmpF trimer in a model membrane. The method described by Antosiewicz is then used to estimate the $pK_a$ of the charged residues of the protein, and therefore their protonation state at a given pH. This allows to calculate the 3-D electric potential distribution inside the channel. This electric potential distribution is then transformed into a 1-D effective charge density profile along the axis. Once this effective charge density is known, the PNP system of equations is solved in a self-consistent manner and the results are compared to experimental data. Our main findings are:

(1) The $pK_a$ determination of all titratable residues in the OmpF channel enables the rationalization of the measured pH dependent selectivity. The successive protonation and deprotonation of acidic and basic residues explains how this cation-selective channel at basic and neutral pH turns into anion-selective in an acidic environment.
(2) The 3-D structural information can be transformed into an effective charge density which can be used as an input for a 1-D electrodiffusion model. It is shown how the reversal potential and conductance measurements under different conditions of concentration and pH can be explained by means of averaged quantities.
(3) Despite its low resolution, the model still captures some special features of the channel: the asymmetry found in the measured selectivity under salt gradient inversion arises naturally as a consequence of the channel structure.
(4) The influence of the charge of the lipids forming the planar membrane can be introduced in the model by assigning an effective charge to the model membrane. The increase of the reversal potential can then attributed to the extra fixed charge contributed by the lipid membrane.
(5) The same methodology can be satisfactorily applied to some OmpF mutants. Electrostatic averages can account for structural reorganizations involving only a small number of amino-acids but a relatively large number of net charges.
(6) The correlation found between atomic structure and ion selectivity shows that the transport characteristics of wide channels like OmpF are mainly regulated by the collective action of a large number of residues, rather than by the specific interactions of residues at particular locations.

## Acknowledgements

This work was supported by Fundació Caixa-Castelló (project P1-1B2004-27), Generalitat Valenciana (project GV04A/701) and from MEC (project FIS2004-03424).

## References

[1] H. Nikaido, Molecular basis of bacterial outer membrane permeability revisited, Microbiol. Mol. Biol. Rev. 67 (2003) 593–656.
[2] A.H. Delcour, Solute uptake through general porins, Front. Biosci. 8 (2003) 1055–1071.
[3] A. Alcaraz, M. Aguilella-Arzo, E.M. Nestorovich, V.M. Aguilella, S.M. Bezrukov, Salting out the ionic selectivity of a wide channel: the asymmetry of OmpF, Biophys. J. 87 (2004) 943–957.
[4] E.M. Nestorovich, C. Danelon, M. Winterhalter, S.M. Bezrukov, Designed to penetrate: time resolved interaction of single antibiotic molecules with bacterial porins, Proc. Natl. Acad. Sci. U. S. A. 99 (2002) 9789–9794.
[5] B. Roux, T. Allen, S. Bernèche, W. Im, Theoretical and computational models of biological ion channels, Q. Rev. Biophys. 37 (2004) 15–103.
[6] D.P. Tieleman, H.J.C. Berendsen, A molecular dynamics study of the pores formed by *Escherichia coli* OmpF porin in a fully hydrated palmitoyloleoylphosphatidylcholine bilayer, Biophys. J. 74 (1998) 2786–2801.
[7] W. Im, B. Roux, Ions and counterions in a biological channel: a molecular dynamics simulation of OmpF porin from *Escherichia coli* in an explicit

membrane with 1 M KCl aqueous salt solution, J. Mol. Biol. 319 (2002) 1177–1197.
[8] W. Im, B. Roux, Ion permeation and selectivity of OmpF porin: a theoretical study based on molecular dynamics, Brownian dynamics and continuum electrodiffusion theory, J. Mol. Biol. 322 (2002) 851–869.
[9] C. Danelon, A. Suenaga, M. Winterhalter, I. Yamato, Molecular origin of the cation selectivity in OmpF porin: single channel conductances vs. free energy calculation, Biophys. Chem. 104 (2003) 591–603.
[10] D.P. Chen, J. Tang, B. Eisenberg, Structure–function study of porins, Technical Proceedings of the 2002 International Conference of Computational Nanoscience and Nanotechnology, Amer Inst of Aeronautics, 2003.
[11] A. Fulinski, I.D. Kosinska, Z. Siwy, Transport properties of nanopores in electrolyte solutions: the diffusional model and surface currents, New J. Phys. 7 (132) (2005) 1–18.
[12] J. Cervera, B. Schiedt, P. Ramírez, A Nernst–Planck/Poisson model for ionic transport through synthetic conical nanopores, Europhys. Lett. 71 (2005) 35–41.
[13] I.D. Kosinka, A. Fulinski, Asymmetric nanodiffusion, Phys. Rev. E 72 (011201) (2005) 1–7.
[14] B. Corry, S. Kuyucak, S.H. Chung, Invalidity of continuum theories of electrolytes in nanopores, Chem. Phys. Lett. 320 (2000) 35–41.
[15] D.G. Levitt, General continuum theory for multiion channel. II. Application to acetylcholine channel, Biophys J. 59 (1991) 278–288.
[16] W. Nonner, B. Eisenberg, Ion permeation and glutamate residues linked by Poisson–Nernst–Planck theory in L-type calcium channels, Biophys. J. 75 (1998) 1287–1305.
[17] D. Chen, L. Xu, A. Tripathy, G. Meissner, B. Eisenberg, Selectivity and permeation in calcium release channel of cardiac muscle: alkali metal ions, Biophys. J. 76 (1999) 1346–1366.
[18] E.B. Zambrowicz, M. Colombini, Zero-current potentials in a large membrane channel: a simple theory accounts for complex behavior, Biophys. J. 65 (1993) 1093–1100.
[19] V. Levadny, V.M. Aguilella, Reversal potential of a wide ion channel. Nonuniform charge distribution effects, J. Phys. Chem. B 105 (2001) 9902–9908.
[20] T. Grasser, T.W. Tang, H. Kosina, S. Selberherr, A review of hydrodynamic and energy-transport models for semiconductor device simulation, Proc. IEEE 91 (2003) 251–274.
[21] C. Jacoboni, P. Lugli, The Monte Carlo Method for Semiconductor Device Simulation, Springer-Verlag, New York, 1989.
[22] S. Selberherr, Analysis and Simulation of Semiconductor Devices, Springer-Verlag, New York, 1984.
[23] S.W. Cowan, T. Schirmer, G. Rummel, M. Steiert, R. Ghosh, R.A. Pauptit, J.N. Jansonius, J.P. Rosenbusch, Crystal structures explain functional properties of two *E. coli* porins, Nature 358 (1992) 727–733.
[24] J. Antosiewicz, J.A. McCammon, M.K. Gilson, Prediction of pH-dependent properties of proteins, J. Mol. Biol. 238 (1994) 415–436.
[25] J. Antosiewicz, J.A. McCammon, M.K. Gilson, The determinants of p$K_{as}$ in proteins, Biochemistry 35 (1996) 7819–7833.
[26] M.E. Davis, J.D. Madura, B.A. Luty, J.A. McCammon, Electrostatics and diffusion of molecules in solution: simulations with the University of Houston Brownian dynamics program, Comp. Phys. Comm. 62 (1991) 187–197.
[27] J.D. Madura, J.M. Briggs, R.C. Wade, M.E. Davis, B.A. Luty, A. Ilin, J. Antosiewicz, M.K. Gilson, B. Bagheri, L.R. Scott, J.A. McCammon, Electrostatics and diffusion of molecules in solution: simulations with the University of Houston Brownian Dynamics Program, Comp. Phys. Comm. 91 (1995) 57–95.
[28] R. Zwanzig, Diffusion past an entropy barrier, J. Phys. Chem. 69 (1992) 3926–3930.
[29] S. Kuyucak, O.S. Andersen, S.H. Chung, Models of permeation in ion channels, Rep. Prog. Phys. 64 (2001) 1427–1472.
[30] S. Varma, Jakobsson, Ionization states of residues in OmpF and mutants: effects of dielectric constant and interactions between residues, Biophys. J. 86 (2004) 690–704.
[31] F. Fogolari, A. Brigo, H. Molinari, The Poisson–Boltzmann equation for biomolecular electrostatics: a tool for structural biology, J. Mol. Recognit. 15 (2002) 377–392.
[32] F. Helfferich, Ion Exchange, McGraw-Hill, New York, 1962.
[33] B. Hille, Ionic Channels of Excitable Membranes, Sinauer, Sunderland, Mass, 2001.
[34] D. Gillespie, R.S. Eisenberg, Modified Donnan potentials for ion transport through biological ion channels, Phys. Rev. E 63 (2001) 061902.
[35] D. Chen, R.S. Eisenberg, Charges, currents and potentials in ionic channels of one conformation, Biophys. J. 64 (1993) 1405–1421.
[36] A. Karshikoff, V. Spassov, S. Cowan, R. Ladenstein, T. Schirmer, Electrostatic properties of two porin channels from *Escherichia coli*, J. Mol. Biol. 240 (1994) 372–384.
[37] E.M. Nestorovich, T.K. Rostovtseva, S.M. Bezrukov, Residue ionization and ion transport through OmpF channels, Biophys. J. 85 (2003) 3718–3729.
[38] T. Schirmer, P. Phale, Brownian dynamics simulation of ion flow through porin channels, J. Mol. Biol. 294 (1999) 1159–1167.
[39] H. Miedema, A. Meter-Arkema, J. Wierenga, J. Tang, B. Eisenberg, W. Nonner, H. Hektor, D. Gillespie, W. Meijberg, Permeation properties of an engineered bacterial OmpF porin containing the EEEE-locus of Ca2+ channels, Biophys. J. 87 (2004) 3137–3147.
[40] D. van der Spoel, E. Lindahl, B. Hess, G. Groenhof, A.E. Mark, H.J.C. Berendsen, GROMACS: fast, flexible, and free, J. Comp. Chem. 26 (2005) 1701–1718.